ELSEVIER

Journal of Physics and Chemistry of Solids 62 (2001) 1813–1818

JOURNAL OF PHYSICS AND CHEMISTRY OF SOLIDS

www.elsevier.com/locate/jpcs

Spin–orbit scattering effect on electron–electron interactions in disordered metals

J.J. Lin[a,*], S.Y. Hsu[b], J.C. Lue[a], P.J. Sheng[a]

[a]*Institute of Physics, National Chiao Tung University, Hsinchu 300, Taiwan*
[b]*Department of Electrophysics, National Chiao Tung University, Hsinchu 300, Taiwan*

Received 10 January 2001; accepted 12 January 2001

Abstract

We have measured the low-temperature resistivities of a series of bulk crystalline disordered $Ti_{73-x}Al_{27}Sn_x$ alloys ($x \lesssim 5$) as well as the sheet resistances of a number of thin ferromagnetic Ni films (≈ 120 Å thick) sandwiching an ultrathin Ag or Au ($\lesssim 5$ Å) layer. The level of impurities (concentration of Sn in the former case, and thickness of Ag or Au in the latter case) is progressively increased in order to enhance the spin–orbit scattering in a controllable manner. The influence of the spin–orbit scattering on the electron–electron interaction effects is studied from the temperature dependence of resistivities (sheet resistance) at low temperatures. We find that the electron–electron interaction contribution to the resistivities (sheet resistances) increases slightly with increasing spin–orbit scattering. Our observation is discussed in terms of the current theoretical concept for the electron–electron interactions in disordered metals.

PACS: 72.15.-v; 72.15.Rn; 73.50-h

1. Introduction

Extensive theoretical and experimental efforts have been made over decades to study the problem of the metal–insulator transition in disordered systems [1]. It is now known that in an interacting electronic system and in the presence of strong disorder, both localization and electron–electron interaction effects are crucial in driving the metal–insulator transition. However, the relative importance of the two effects is still not very clear. Efforts to investigate the individual contributions from the two effects are, therefore, of fundamental significance and interest. In this work, we have carefully fabricated two different weakly disordered metallic systems in order to study the corrections to the low-temperature resistances (or, more precisely, resistivities in three dimensions and sheet resistances in two dimensions) due to electron–electron interaction effects. One example system consists of bulk crystalline disordered $Ti_{73-x}Al_{27}Sn_x$ alloys with $x \lesssim 5$ (hereafter, referred to as TiAlSn). The other sample system consists of thin Ni films sandwiching an ultrathin (impurity) layer of either Ag or Au. The former sample system is three-dimensional (3D) and hence the temperature dependence of the low-temperature resistivity in the absence of a magnetic field arises mainly from the disorder enhanced electron–electron interaction effects [2,3]. The latter sample system is two-dimensional (2D). It is known that, in general, both weak-localization and electron–electron interaction effects could contribute significantly to the temperature dependence of the low-temperature sheet resistance in 2D. Nevertheless, due to the ferromagnetic nature of the host material (Ni) being detrimental to weak-localization effects [4], the temperature dependence of the low-temperature sheet resistance is, thus, also dominated only by electron–electron interaction effects in the latter sample system.

Experimentally, the influence of spin–orbit scattering on disorder enhanced electron–electron interaction effects have previously been studied by high-field magnetoresistance measurements [5,6]. The Coulomb screening parameter $\tilde{F}$, defined in the e–e interaction theory, is then extracted by comparing the measured magnetoresistance with the sum of the theoretical weak-localization magnetoresistance plus

* Corresponding author. Tel.: +886-3-5731652; fax: +886-3-5720728.

E-mail address: jjlin@cc.nctu.edu.tw (J.J. Lin).

0022-3697/01/$ - see front matter
PII: S0022-3697(01)00113-5

theoretical electron–electron interaction magnetoresistance. Technically, this method involves *several* adjustable parameters in the least-squares fits of the experimental data with theory; and, hence, is not a very desirable way of extracting the value of $\tilde{F}$. In this work, we have studied the variation of $\tilde{F}$ with the spin–orbit scattering rate, τ_{so}^{-1} by measuring the temperature dependence of the resistance in zero magnetic field. Here, the low-temperature resistance is solely controlled by the electron–electron interaction effects, as just mentioned. Therefore, the number of fitting parameters is greatly reduced and, in fact, there is now only *one* free parameter involved in the comparison of experimental data with theory, namely, $\tilde{F}$. Our results for the variation of $\tilde{F}$ with τ_{so}^{-1} are reported below.

2. Theory

Altshuler and coworkers have calculated the corrections to low-temperature resistivities and sheet resistances due to electron–electron interaction effects in the weakly disordered regime and predicted that [2]

$$\frac{\Delta\rho(T)}{\rho_0} = \frac{\rho(T)-\rho_0}{\rho_0} = -\frac{0.915e^2}{4\pi^2\hbar}\left(\frac{4}{3}-\frac{3}{2}\tilde{F}^{(3D)}\right)\rho_0\sqrt{\frac{k_BT}{\hbar D}} \quad (1)$$

in three dimensions, where ρ_0 is a reference low-temperature resistivity [taken to be $\rho_0=\rho(10\text{ K})$ in this work], D is the electron diffusion constant, and the Coulomb screening parameter is explicitly denoted by $\tilde{F}^{(3D)}$. They have also predicted that

$$\frac{\Delta G(T)}{G_{00}} = \frac{G(T)-G(T_0)}{G_{00}} = (1-\tilde{F}^{(2D)})\ln\left(\frac{T}{T_0}\right) \quad (2)$$

in two dimensions, where T_0 is a reference temperature, $G_{00}=e^2/2\pi^2\hbar$ is the quantum conductance, and the Coulomb screening parameter is explicitly denoted by $\tilde{F}^{(2D)}$. In Eqs. (1) and (2), the parameter $\tilde{F}^{(3D)}$ or $\tilde{F}^{(2D)}$ is a measure of the screened Coulomb interaction. These correction terms stem from the diffusion channel involving small momentum and frequency transfers. Physically, there is a suppression of the single-electron density of states at the Fermi level caused by the enhanced electron–electron interactions in the presence of disorder. Such a suppression has been confirmed experimentally by tunneling electronic density of states measurements [7,8].

According to the theory, the electron screening parameter $\tilde{F}$ ($\tilde{F}^{(3D)}$ or $\tilde{F}^{(2D)}$) is a measure of F (defined in the e–e interaction theory) which is the dimensionless screened Coulomb potential between electrons averaged over the Fermi surface [2]. Within the Thomas–Fermi approximation, $F\rightarrow 1$ in the limit of complete screening (or, good metals), while $F\rightarrow 0$ in the limit of no screening (or, 'bad' conductors). Eqs. (1) and (2) suggest that poor screening of electrons due to large interaction effects causes a significant rise of low-temperature resistivity (sheet resistance). In general $\tilde{F}\approx F$ in the limit $F\ll 1$. If F is not small, it can be readily shown that $\tilde{F}$ equals F to within $\approx 10\%$ for F in the range $|F|\leq 1$. Thus, it should not be critical to distinguish between $\tilde{F}$ and F in most experiments, including the present work discussed below. An explicit expression for the relation between $\tilde{F}$ and F can be found in Refs. [2,3].

The screening parameter $\tilde{F}$($\tilde{F}^{(3D)}$ or $\tilde{F}^{(2D)}$) is one of the most important, yet not very well understood parameters defined by the electron–electron interaction theory [2]. Because of the enormously complicated interaction effects between electrons, the magnitude of $\tilde{F}$ in a real disordered material is extremely difficult to calculate theoretically. In the presence of spin–flip scattering (spin–orbit scattering and spin–spin scattering), the situation becomes even less clear. It has been argued that the contribution from the diffusion channel to electron–electron interaction effects would be suppressed in the presence of strong spin–orbit scattering [9,10]. This prediction has not attracted much experimental attention thus far, compared with, for example, the very extensively studied weak-localization predictions for magnetoresistance.

3. Experimental method

In order to study the spin–orbit scattering effect on electron–electron interactions, we have fabricated two series of samples in this work. The two sample systems have significantly different material characters.

(i) A series of bulk crystalline disordered $Ti_{73-x}Al_{27}Sn_x$ ($x\lesssim 5$) alloys were fabricated by a standard arc-melting method [11]. Impurity Sn atoms were progressively introduced into the parent $Ti_{73}Al_{27}$ phase to 'tune' the strength of the spin–orbit scattering in a controllable manner, while leaving the amounts of disorder of the samples barely changed. That is, the residual resistivities of our alloys are essentially the same, with $\rho_0=\rho(10\text{ K})\approx 225\ \mu\Omega$ cm, corresponding to an electron mean free path already in the limit of the interatomic spacing. Thus, further doping of Sn into the parent $Ti_{73}Al_{27}$ phase can hardly change or increase ρ_0. X-ray diffraction measurements confirmed that all of our ternary alloy samples possessed a structure similar to that of the parent $Ti_{73}Al_{27}$ phase. The alloys were cut into rectangular shapes, typically $0.2\times 1\times 10\text{ mm}^3$, for four-probe resistance measurements.

The parent $Ti_{73}Al_{27}$ phase is chosen because Ti possesses a moderately small atomic number $Z=22$, while Al has an even smaller atomic number $Z=13$. Therefore, the spin–orbit scattering is expected to be moderately weak in this alloy, leaving plenty of room for increasing the spin–orbit scattering rate, τ_{so}^{-1}, by 'controlled' doping of heavy atoms. This is one of the reasons why Sn is used as the impurity atom, as Sn has atomic number $Z=50$. Notice that this $Z=50$ is sufficiently heavier than that of Ti while it is still not as large as that of, for example, Au ($Z=79$) or Bi ($Z=83$). Since it is known that τ_{so}^{-1} increases rapidly with increasing atomic

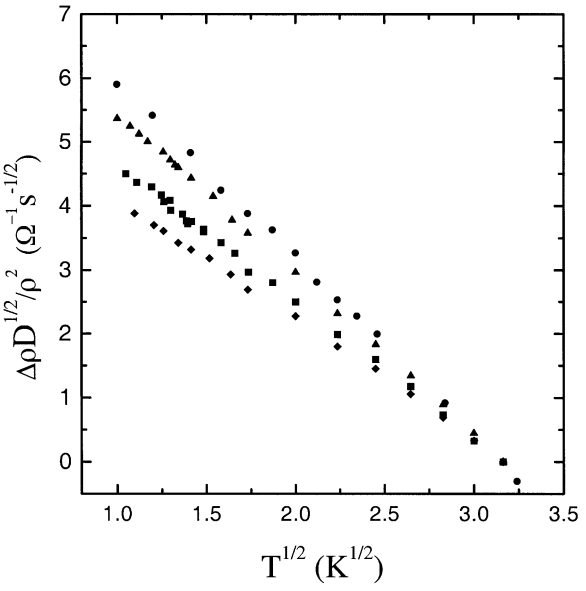

Fig. 1. The normalized resistivities $\Delta\rho\sqrt{D}/\rho^2$ as a function of $\sqrt{T}$ for four representative $Ti_{73-x}Al_{27}Sn_x$ alloys with $x \approx 1.0$ (diamonds), 1.5 (squares), 3.0 (triangles), and 5.0 (circles).

number as $\tau_{so}^{-1} \sim Z^4$ [12], a small amount of Sn doping will, thus, on the one hand, significantly increase τ_{so}^{-1}, while, on the other hand, leave the degree of disorder ρ_0 unchanged as just mentioned. Consequently, any change in $\tilde{F}^{(3D)}$ in this experiment, if observed, should result from enhanced spin–orbit scattering instead of from the change in disorder. If Au or Bi were used as the impurity atoms, it would be much harder to 'tune' the magnitude of τ_{so}^{-1} step by step (see Fig. 2), because a very minute amount of Au or Bi doping would likely have already pushed the system into the limit of strong spin–orbit scattering ($\tau_{so}^{-1} \gg \tau_{\phi}^{-1}$, the electron dephasing rate) where τ_{so}^{-1} cannot be accurately extracted from the weak-localization theoretical predictions [13].

The value of the electron diffusion constant D for our alloys is evaluated through the Einstein relation $\rho_0^{-1} = N(0)e^2D$, where ρ_0 is the measured residual resistivity, and $N(0)$ is the electronic density of states at the Fermi level deduced from specific heat measurement at liquid helium temperatures. We obtain $D \approx 0.85\ \mathrm{cm}^2/\mathrm{s}$ for *all* our alloys with the same $\rho_0 \approx 225\ \mu\Omega$ cm [11].

(ii) Two dimensional Ni films doped with an ultrathin layer of Ag or Au were prepared by in situ sequent thermal evaporation in a vacuum of $\lesssim 5 \times 10^{-6}$ torr on glass substrates held at room temperatures. The ultrathin impurity Ag or Au layer ($\lesssim 5$ Å) was deposited mid-way between two 60-Å thick Ni layers to form a sandwiched sample. The deposition rates for the host Ni and impurity layers were about 0.4 and 0.014 Å/s, respectively. The strength of the spin–orbit scattering in the samples was increased gradually by systematically increasing the thickness of the ultrathin impurity layer.

Low-temperature resistance measurements were conducted using an ac resistance bridge and a ^{3}He cryostat. The temperature was monitored with a calibrated RuO_2 and a calibrated carbon–glass thermometer.

4. Results

4.1. $Ti_{73-x}Al_{27}Sn_x$ alloys

In a three-dimensional weakly disordered system at liquid helium temperatures, the resistivity is expected to increase with decreasing temperature with the square root of temperature due to electron–electron interaction effects, Eq. (1). In Fig. 1, we show a plot of the normalized resistivities, $\Delta\rho\sqrt{D}/\rho^2$, as a function of $\sqrt{T}$ for four representative TiAlSn alloys with the concentration of Sn as indicated in the caption to Fig. 1. Here, data are plotted in such a way as to be directly compared with the theoretical prediction of Eq. (1). Inspection of Fig. 1 illustrates that our samples reveal electrical resistivities as caused by disorder enhanced electron–electron interaction effects. That is, the resistivities increase with the square root of temperature below 10 K. On the other hand, there is negligible (less than 5%, see for example, Ref. [14]) contribution from weak-localization effects. If the weak-localization contribution were not negligible, a deviation from $\sqrt{T}$ dependence would have been observed.

The slope of a linear fit to our data in Fig. 1 gives the size of the resistivity corrections, and, thus, the value of the screening parameter $\tilde{F}^{(3D)}$ for each sample. Fig. 1 clearly shows that the slope increases, and, correspondingly, $\tilde{F}^{(3D)}$ decreases with increasing concentration of Sn. In other

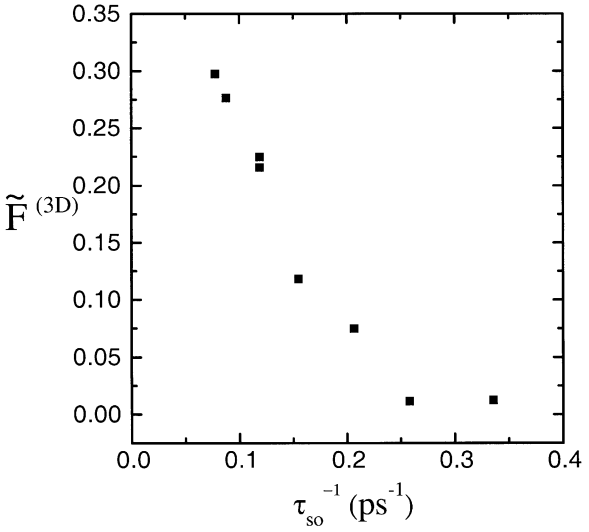

Fig. 2. Variation of $\tilde{F}^{(3D)}$ with spin–orbit scattering rate τ_{so}^{-1} for several $Ti_{73-x}Al_{27}Sn_x$ alloys.

words, $\tilde{F}^{(3D)}$ decreases with increasing spin–orbit scattering. Quantitatively, the variation of $\tilde{F}^{(3D)}$ with the spin–orbit scattering rate, τ_{so}^{-1}, for our TiAlSn samples are plotted in Fig. 2. Fig. 2 demonstrates that $\tilde{F}^{(3D)}$ decreases monotonically with increasing τ_{so}^{-1}. As τ_{so}^{-1} increases from about 7×10^{10} to about 2.5×10^{11} s^{-1}, the value of $\tilde{F}^{(3D)}$ decreases from about 0.31 to 0.01. $\tilde{F}^{(3D)}$ remains *positive* and almost 0 with further increase of τ_{so}^{-1}. Here our spin–orbit scattering rates are determined from weak-localization studies of magnetoresistivities [11,14]. Physically, the decrease in $\tilde{F}^{(3D)}$, as just observed, arises from the diffusion channel being suppressed in the presence of strong spin–orbit scattering [9,10]. Our observation of Fig. 2 is qualitatively, but not quantitatively (see below), in line with this current theoretical understanding.

4.2. Thin Ni films

In a two-dimensional weakly disordered system at liquid helium temperatures, the sheet resistance is expected to increase with decreasing temperature with a functional form of $\ln T$ due to electron–electron interaction effects, Eq. (2). (We ignore the weak-localization contribution as discussed in the Introduction.) In Fig. 3, the normalized conductance, $\Delta G/G_{00}$, as a function of the logarithm of temperature for a representative sandwiched Ni(60 Å)/Au(5 Å)/Ni(60 Å) film is plotted. Here, data (symbols) are plotted in such a way as to be directly compared with the theoretical predictions of Eq. (2) (solid straight line). In this figure, the slope of a linear fit, $A = 1 - \tilde{F}^{(2D)}$, directly yields the value of $\tilde{F}^{(2D)}$ for each sample. We have determined the values of A for several sandwiched Ni/(Ag,Au)/Ni films. Fig. 4 shows the variation of A with the thickness, t, of the ultrathin impurity layer: Ag (squares) or Au (circles). This figure shows that A changes only very slightly ($\lesssim 5\%$) with increasing t. However, it is clear that A increases essentially linearly with t. In other words, A increases, or, correspondingly, $\tilde{F}^{(2D)}$ decreases with increasing spin–orbit scattering. For a given t, the magnitude of A is larger for Au-doped films than for Ag-doped films. This behavior is readily understood in terms of impurity Au atoms being heavier than impurity Ag atoms and, hence, causing a stronger spin–orbit scattering effect on the suppression of $\tilde{F}^{(2D)}$. Therefore, our observation suggests that spin–orbit scattering has a positive, although small, contribution to the electron–electron interaction resistance rises in 2D disordered systems. This assertion of a spin–orbit scattering effect in enhancing the electron–electron interaction resistance corrections hold true in both three- (Fig. 2) and two-dimensional (Fig. 4) cases.

It is worth noting that we have not determined the value of τ_{so}^{-1} in our sandwiched thin Ni films, because the low-temperature magnetoresistance of these ferromagnetic films are *not* caused by weak-localization effects. Instead, the alignment effect of permanent moments in the presence of an externally applied magnetic field dominates the magnetoresistance. Therefore, the values of τ_{so}^{-1} cannot be inferred by the standard weak-localization magnetoresistance measurements.

5. Discussion and conclusion

The main results of this work, Figs. 2 and 4, clearly establish that spin–orbit scattering enhances electron–electron interactions in disordered metals. Similar observations have been reported previously in disordered systems, particularly in bulk metallic glasses. Sahnoune et al. [5,6] and

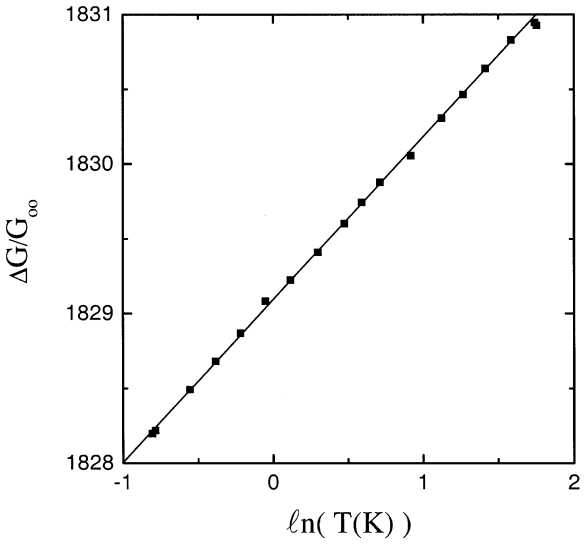

Fig. 3. Normalized sheet conductance $\Delta G/G_{00}$ as a function of ln T for the sandwiched Ni(60 Å)/Au(5 Å)/Ni(60 Å) film. The straight line is a least-squares fit to Eq. (2).

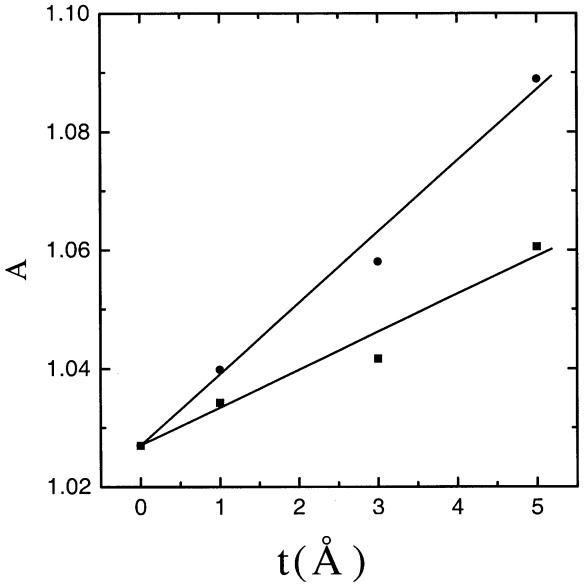

Fig. 4. Variation of $A = 1 - \tilde{F}^{(2D)}$ with the thickness t of impurity Ag layer (squares) or Au layer (circles) for sandwiched Ni(60 Å)/(Ag, Au)/Ni(60 Å) films. The straight solid lines are guides to the eye.

other authors [15,16] have reported that the value of $\tilde{F}^{(3D)}$ decreased for higher spin–orbit scattering rate τ_{so}^{-1} in various amorphous metals. They also found that $\tilde{F}^{(3D)}$ might even become negative in materials with sufficiently large τ_{so}^{-1} ($\gtrsim 10^{12}\,s^{-1}$). Very similar conclusions have also been drawn for bulk polycrystalline metal alloys [3,17]. Such a systematic change of $\tilde{F}^{(3D)}$ with τ_{so}^{-1} cannot be satisfactorily explained by the current electron–electron interaction theory. For example, Altshuler et al. [9] only predict that the $(3/2)\tilde{F}^{(3D)}$ term in Eq. (1) should be replaced by $(3/8)\tilde{F}^{(3D)}$ in the limit of strong spin–orbit scattering. (This means that the triplet part of the electron–electron interaction in the diffusion channel is suppressed.) However, no explicit expression is given for the dependence of $\tilde{F}^{(3D)}$ on τ_{so}^{-1}. On the other hand, to the best of our knowledge, no experimental observation of the dependence of $\tilde{F}^{(2D)}$ on τ_{so}^{-1} has been reported in the literature.

In Fig. 4, our experimental value of A is larger than unity,

suggesting a *negative* $\tilde{F}^{(2D)}$ in our sandwiched thin Ni films. This result is not consistent with the free-electron-model prediction of $\tilde{F}^{(2D)}$, where $\tilde{F}^{(2D)}$ is expected to be always positive. In fact, negative values of $\tilde{F}^{(2D)}$ in thin layers of Ni have been reported previously by Kobayashi et al. [18]. This issue of a negative $\tilde{F}^{(2D)}$ in thin ferromagnetic Ni films still remains open.

In conclusion, we have measured the electron–electron interaction corrections to the low-temperature resistivities of three-dimensional TiAlSn alloys and the sheet resistance of two-dimensional Ni/(Ag,Au)/Ni films. We observe that strong spin–orbit scattering enhances the electron–electron interaction corrections to the resistivities (sheet resistances). This result is not fully theoretically understood.

Acknowledgements

The authors are grateful to R. Rosenbaum for valuable discussion. This work was supported by the Taiwan National Science Council through Grants Nos. NSC 89-2112-M-009-014 and NSC 89-2112-M-009-033.

References

[1] D. Belitz, T.R. Kirkpatrick, The Anderson–Mott transition, Rev. Mod. Phys. 66 (1994) 261–380.
[2] B.L. Altshuler, A.G. Aronov, in: A.L. Efros, M. Pollak (Eds.), Electron–Electron Interactions in Disordered Systems, Elsevier, Amsterdam, 1985, p. 1.
[3] C.Y. Wu, W.B. Jian, J.J. Lin, Phonon-induced electron–electron interaction in disordered superconductors, Phys. Rev. B 52 (1995) 15479–15484.
[4] P.A. Lee, Scaling studies of localization, , J. Non-Crys. Solids, 35– 36 (1980) 21–28.
[5] A. Sahnoune, J.O. Ström-Olsen, H.E. Fischer, Influence of spin–orbit scattering on the magnetoresistance due to enhanced electron–electron interactions, Phys. Rev. B 46 (1992) 10035–10040.
[6] P. Lindqvist, Ö. Rapp, A. Sahnoune, J.O. Ström-Olsen, Magnetoresistance due to enhanced electron–electron interactions in amorphous $Ca_{70}(Mg,Al)_{30}$, Phys. Rev. B 41 (1990) 3841–3843.
[7] R.C. Dynes, J.P. Garno, Metal–insulator transition in granular aluminum, Phys. Rev. Lett. 46 (1981) 137–140.
[8] A.E. White, R.C. Dynes, J.P. Garno, Correction to the two-dimensional density of states, Phys. Rev. B 31 (1985) 1174–1176.
[9] B.L. Altshuler, A.G. Aronov, A.Yu Zuzin, Spin relaxation and interaction effects in the disordered conductors. Solid State Commun. 44 (1982) 137–139.
[10] A.J. Millis, P.A. Lee, Spin–orbit and paramagnon effects on magnetoresistance and tunneling, Phys. Rev. B 30 (1984) 6170–6173.
[11] S.Y. Hsu, P.J. Sheng, J.J. Lin, Quadratic temperature dependence of the electron–phonon scattering rate in disordered metals, Phys. Rev. B 60 (1999) 3940–3943.
[12] A.A. Abriksov, L.P. Gorkov, Spin–orbit interaction and the Knight shift in superconductors, Sov. Phys. JETP 15 (1962) 752–757.
[13] H. Fukuyama, K. Hoshino, Effect of spin–orbit interaction on magnetoresistance in the weakly localized regime of three-dimensional disordered systems, J. Phys. Soc. Jpn. 50 (1981) 2131–2132.
[14] C.Y. Wu, J.J. Lin, Weak-localization and Maki–Thompson superconducting fluctuation effects in crystalline disordered Ti–Al– (Sn,Co) alloys at $T > T_c$, Phys. Rev. B 50 (1994) 385–394.
[15] S.J. Poon, K.M. Wong, A.J. Drehman, Localization and electron–electron interaction effects in metallic glasses, Phys. Rev. B 31 (1985) 1668–1670.
[16] F.M. Mayeya, M.A. Howson, Quantum interference and electron interaction effects in CaAl(Au,Ag) amorphous alloys, J. Phys.: Condens. Matter 4 (1992) 9355–9366.
[17] W.B. Jian, C.Y. Wu, Y.L. Chuang, J.J. Lin, Electron–electron interaction and normal-state transport in superconducting Ti–(Sn,Ge) alloys, Phys. Rev. B 54 (1996) 4289–4292.
[18] S. Kobayashi, Y. Ootuka, F. Komori, W. Sasaki, ln T term and magnetic field effect in conductivity of Ni thin film, J. Phys. Soc. Jpn. 51 (1982) 689–690.